Control of a Five-phase Synchronous Motors with Third Harmonic Constrained Injection.

Marco Fei and Roberto Zanasi

***Abstract*— This paper deals with the torque control of five-phase permanent magnet synchronous machines with first and third harmonics injection. A new vectorial approach to describe the voltage and current limits is proposed. Starting from the transformed dynamic equations and using the voltage and current constraints, the optimal current references minimizing the dissipation and maximizing the torque is obtained. The proposed control law holds for an arbitrary shape of the rotor flux. Some simulation results validate the proposed control law.**

I. INTRODUCTION

Multi-phase machines posses many advantages over the three-phase machines as the higher torque-to-volume ratio due to the injection of higher order current harmonics for the machines with concentrated winding and nearly rectangular back-emf, see [1], [2] and [3]. In [4] and [5] the effects of the voltage and current limits on the third harmonic injection are considered. Although the amplitude of the injected harmonics is tied to the harmonic spectrum of the back-emf, it is not clear in the cited papers how the current references are obtained.

This paper uses a new vectorial approach to obtain the optimal current references considering the voltage and current limits. The paper is organized as follows. Sec. II shows the details of the dynamic model of the 5-phase synchronous motors. In Sec. III the current and voltage constraints are considered and their effects onto the torque producing capability are shown in Sec. IV. The proposed torque control is given in Sec. V. Some simulation results are presented in Sec. VI and conclusions are given in Sec. VII.

II. ELECTRICAL MOTORS MODELING

The basic structure of a permanent magnet synchronous motor with five concentrated winding in star connection is shown in Fig. 1 and its parameters are shown in Tab. 2. A complex and reduced model expressed in the rotating frame $\overline{\Sigma}_\omega$ can be obtained using the following complex transformation matrix ${}^t\overline{\mathbf{T}}_{\omega N}$, see [7]:

$${}^t\overline{\mathbf{T}}^*_{\omega N}=\sqrt{\frac{2}{5}}\begin{bmatrix} e^{-j\theta} & e^{j(\gamma_s-\theta)} & e^{j(2\gamma_s-\theta)} & e^{j(3\gamma_s-\theta)} & e^{j(4\gamma_s-\theta)} \\ e^{-j3\theta} & e^{j3(\gamma_s-\theta)} & e^{j3(2\gamma_s-\theta)} & e^{j3(3\gamma_s-\theta)} & e^{j3(4\gamma_s-\theta)} \end{bmatrix}$$

The transformed system $\overline{S}_\omega$ expressed in the complex reduced rotating frame $\overline{\Sigma}_\omega$ has the following form:

$$\left[\begin{array}{c|c} {}^\omega\overline{\mathbf{L}}_s & \mathbf{0} \\ \hline \mathbf{0} & J_m \end{array}\right]\begin{bmatrix} {}^\omega\dot{\overline{\mathbf{I}}}_s \\ \dot{\omega}_m \end{bmatrix}=-\left[\begin{array}{c|c} {}^\omega\overline{\mathbf{Z}}_s & {}^\omega\overline{\mathbf{K}}_{\tau N} \\ \hline -{}^\omega\overline{\mathbf{K}}^*_{\tau N} & b_m \end{array}\right]\begin{bmatrix} {}^\omega\overline{\mathbf{I}}_s \\ \omega_m \end{bmatrix}+\begin{bmatrix} {}^\omega\overline{\mathbf{V}}_s \\ -\tau_e \end{bmatrix}. \quad (1)$$

M. Fei and R. Zanasi are with the Information Engineering Department, University of Modena and Reggio Emilia, Via Vignolese 905, 41100 Modena, Italy, e-mail: {marco.fei, roberto.zanasi}@unimore.it.

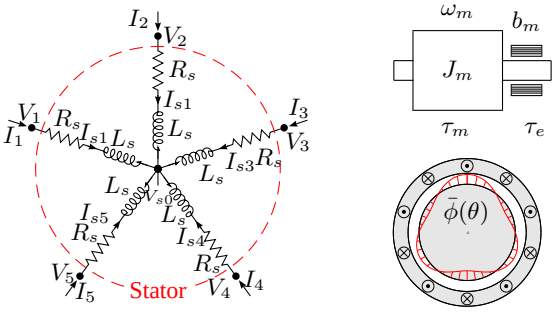

Fig. 1. Basic structure of a star-connected five-phase synchronous motor.

m_s	number of motor phases: $m_s = 5$
p	number of polar expansions
θ, θ_m	electric and rotor angular positions: $\theta = p\,\theta_m$
ω, ω_m	electric and rotor angular velocities: $\omega = p\,\omega_m$
R_s	i-th stator phase resistance
L_s	i-th stator phase self induction coefficient
M_{s0}	maximum value of the stator mutual inductance
M_{hi}	mutual induction coefficient of h-th and i-th phases: $M_{hi} = M_{s0}[a_{M1}\cos((h-i)\gamma_s) + a_{M3}\cos(3(h-i)\gamma_s)]$
J_m	rotor moment of inertia
b_m	rotor linear friction coefficient
τ_m	electromotive torque acting on the rotor
τ_e	external load torque acting on the rotor
γ_s	basic angular displacement ($\gamma_s = 2\pi/5$)
$\phi_c(\theta)$	total rotor flux chained with stator phase 1
φ_c	maximum value of function $\phi_c(\theta)$
$\bar{\phi}(\theta)$	normalized rotor flux: $\bar{\phi}(\theta) = \dfrac{\phi_c(\theta)}{\varphi_c} = \sum_{n=1:2}^{\infty} a_i \cos(n\,\theta)$

Fig. 2. Parameters of the multi-phase synchronous motor.

Fig. 3 shows how the original 5-dimension model $\overline{S}_t$ in the fixed frame Σ_t has been transformed and reduced to a 2-dimension complex model $\overline{S}_\omega$ in the rotating frame $\overline{\Sigma}_\omega$. In this frame the 5-phase motor can be seen as a set of 2 independent electrical machines rotating at velocity ω_m and $3\omega_m$ within the complex subspaces $\overline{\Sigma}_{\omega 1}$ and $\overline{\Sigma}_{\omega 3}$, respectively. The dynamic equations of the electrical part of system (1) are equivalent to the following two equations defined in the complex subspaces $\overline{\Sigma}_{\omega k}$ with $k \in \{1, 3\}$:

$$L_{sk}\dot{\overline{I}}_{sk} = -(R_s + jp\,\omega_m\,L_{sk})\overline{I}_{sk} - \overline{K}_{\tau k}\omega_m + \overline{V}_{sk} \quad (2)$$

where: $L_{sk} = L_s + M_{s0}\left(\frac{m_s}{2}a_{Mk} - 1\right)$. Note that, according to [2], the first two odd components $a_{M1}M_{s0}$ and $a_{M3}M_{s0}$ of the mutual inductance (see Tab. 2) are explicitly considered. The components $\overline{K}_{\tau 1}$ and $\overline{K}_{\tau 3}$ of torque vector ${}^\omega\overline{\mathbf{K}}_{\tau N}$ are function of the coefficients a_n of the rotor flux Fourier series shown in Tab. 2. In this paper only the coefficients a_1 and a_3 of the normalized rotor flux $\bar{\phi}$ are considered, so the

$$\left[\begin{array}{cc|c} L_{s1} & 0 & 0 \\ 0 & L_{s3} & 0 \\ \hline 0 & 0 & J_m \end{array}\right]\left[\begin{array}{c} \dot{\overline{I}}_{s1} \\ \dot{\overline{I}}_{s3} \\ \hline \dot{\omega}_m \end{array}\right] = -\left[\begin{array}{cc|c} R_s + jp\,\omega_m\,L_{s1} & 0 & jp\varphi_c\sqrt{\frac{5}{2}}\,a_1 \\ 0 & R_s + j\,3\,p\,\omega_m\,L_{s3} & jp\varphi_c\sqrt{\frac{5}{2}}\,3\,a_3 \\ \hline -\,jp\varphi_c\sqrt{\frac{5}{2}}\,a_1 & -jp\varphi_c\sqrt{\frac{5}{2}}\,3\,a_3 & b_m \end{array}\right]\left[\begin{array}{c} \overline{I}_{s1} \\ \overline{I}_{s3} \\ \hline \omega_m \end{array}\right] + \left[\begin{array}{c} \overline{V}_{s1} \\ \overline{V}_{s3} \\ \hline -\,\tau_e \end{array}\right]$$

Fig. 3. Dynamic model of star-connected 5-phase synchronous motors in the reduced complex rotating frame $\overline{\Sigma}_\omega$.

components $\overline{K}_{\tau 1}$ and $\overline{K}_{\tau 3}$ are constant, see [9]:

$$^{\omega}\overline{\mathbf{K}}_{\tau N} = \begin{bmatrix} \overline{K}_{\tau 1} \\ \overline{K}_{\tau 3} \end{bmatrix} = \begin{bmatrix} K_{d1} + jK_{q1} \\ K_{d3} + jK_{q3} \end{bmatrix} = jp\varphi_c\sqrt{\frac{5}{2}}\begin{bmatrix} a_1 \\ 3a_3 \end{bmatrix}. \quad (3)$$

The motor torque τ_m and the transformed back-electromotive force $^{\omega}\overline{\mathbf{E}}$ are:

$$\tau_m = \mathfrak{Re}\left(^{\omega}\overline{\mathbf{K}}^{*}_{\tau N}\,^{\omega}\overline{\mathbf{I}}_s\right), \quad ^{\omega}\overline{\mathbf{E}} = {}^{\omega}\overline{\mathbf{K}}_{\tau N}\omega_m. \quad (4)$$

In [1] and [2] it is shown that it is possible to increase the motor torque of a multi phase motor by injecting odd harmonics with order below m_s. Let us now consider the case of balanced voltage and current stator vectors $^{t}\mathbf{V}_s$ and $^{t}\mathbf{I}_s$ composed only by the first and third harmonics. The phase voltages V_{sh} and the phase currents I_{sh} with $h \in \{0:4\}$ are:

$$V_{sh} = V_{m1}\cos(\theta - (\theta_{v1} - h\gamma_s)) + V_{m3}\cos(3\theta - 3(\theta_{v3} - h\gamma_s)), \quad (5)$$

$$I_{sh} = I_{m1}\cos(\theta - (\theta_{i1} - h\gamma_s)) + I_{m3}\cos(3\theta - 3(\theta_{i3} - h\gamma_s)), \quad (6)$$

where θ_{v1}, θ_{v3}, θ_{i1} and θ_{i3} are proper initial phase shifts. The transformed vectors $^{\omega}\overline{\mathbf{V}}_s = {}^{t}\overline{\mathbf{T}}^{*}_{\omega N}\,{}^{t}\mathbf{V}_s$ and $^{\omega}\overline{\mathbf{I}}_s = {}^{t}\overline{\mathbf{T}}^{*}_{\omega N}\,{}^{t}\mathbf{I}_s$ have the following structure:

$$^{\omega}\overline{\mathbf{V}}_s = \begin{bmatrix} \overline{V}_{s1} \\ \overline{V}_{s3} \end{bmatrix} = \begin{bmatrix} V_{d1} + jV_{q1} \\ V_{d3} + jV_{q3} \end{bmatrix} = \sqrt{\frac{5}{2}}\begin{bmatrix} V_{m1}\,e^{j\theta_{v1}} \\ V_{m3}\,e^{j3\theta_{v3}} \end{bmatrix} \quad (7)$$

$$^{\omega}\overline{\mathbf{I}}_s = \begin{bmatrix} \overline{I}_{s1} \\ \overline{I}_{s3} \end{bmatrix} = \begin{bmatrix} I_{d1} + jI_{q1} \\ V_{I3} + jI_{q3} \end{bmatrix} = \sqrt{\frac{5}{2}}\begin{bmatrix} I_{m1}\,e^{j\theta_{i1}} \\ I_{m3}\,e^{j3\theta_{i3}} \end{bmatrix} \quad (8)$$

where I_{dk}, I_{qk}, V_{dk} and V_{qk} are, respectively, the *direct* and *quadrature* components of the current and voltage vectors $\overline{I}_{sk}$ and $\overline{V}_{sk}$. Expressions (7) and (8) show that the first harmonics of amplitude V_{m1} and I_{m1} in (5) and (6) are transformed into vectors $\overline{V}_{s1}$ and $\overline{I}_{s1}$ with modulus $V_{M1} = \sqrt{\frac{m_s}{2}}V_{m1}$ and $I_{M1} = \sqrt{\frac{m_s}{2}}I_{m1}$ which move within the complex subspace $\overline{\Sigma}_{\omega 1}$, while the third harmonics of amplitude V_{m3} and I_{m3} are transformed into vectors $\overline{V}_{s3}$ and $\overline{I}_{s3}$ with modulus $V_{M3} = \sqrt{\frac{m_s}{2}}V_{m3}$ and $I_{M3} = \sqrt{\frac{m_s}{2}}I_{m3}$ which move within the complex subspace $\overline{\Sigma}_{\omega 3}$. Substituting (3) and (8) in (4) the motor torque can be rewritten as:

$$\tau_m = p\varphi_c\sqrt{\frac{m_s}{2}}\left[a_1 I_{q1} + 3a_3 I_{q3}\right]. \quad (9)$$

This equation shows the dependence of torque τ_m on the quadrature components I_{q1} and I_{q3} of the current vectors $\overline{I}_{s1}$ and $\overline{I}_{s3}$. From (9) it is clear that the torque production capability of the machine increases injecting also the third harmonic. Moreover it shows that the motor torque is generated by the interaction between the harmonics a_k of the rotor flux and the stator current harmonic with the same order k. According to this the amplitude of the injected harmonics is tied to the harmonic spectrum of the rotor flux: it is useless to apply high I_{qk} in subspaces with low components ka_k.

III. MULTI HARMONICS CONSTRAINTS

The amplitudes of components V_{sh} and I_{sh} of the voltage and current vectors $^{t}\mathbf{V}_s$ and $^{t}\mathbf{I}_s$ in (5) and (6) are bounded, respectively, by the maximum voltage V_{max} of the inverter DC link and the maximum rated current I_{max}, therefore the following constraints hold:

$$V_{m1} + V_{m3} \le V_{max}, \qquad I_{m1} + I_{m3} \le I_{max}. \quad (10)$$

Let us define the vectors $\mathbf{V}_M$, $\mathbf{I}_M$ and $\mathbf{K}_\tau \in \mathbb{R}^2$ as:

$$\mathbf{V}_M = \begin{bmatrix} |\overline{V}_{s1}| \\ |\overline{V}_{s3}| \end{bmatrix}, \quad \mathbf{I}_M = \begin{bmatrix} |\overline{I}_{s1}| \\ |\overline{I}_{s3}| \end{bmatrix}, \quad \mathbf{K}_\tau = \begin{bmatrix} |\overline{K}_{\tau 1}| \\ |\overline{K}_{\tau 3}| \end{bmatrix}. \quad (11)$$

The voltage and current constraints (10), multiplied by constant $\sqrt{\frac{m_s}{2}}$, can be rewritten as a 1-norm constraints on vectors $\mathbf{V}_M$ and $\mathbf{I}_M$:

$$\|\,\mathbf{V}_M\,\|_1 = V_{M1} + V_{M3} \le \sqrt{\frac{5}{2}}\,V_{max} = V_{\overline{M}}, \quad (12)$$

$$\|\,\mathbf{I}_M\,\|_1 = I_{M1} + I_{M3} \le \sqrt{\frac{5}{2}}\,I_{max} = I_{\overline{M}}. \quad (13)$$

In the design of the control law there are some degrees of freedom that will be used to distribute the maximum voltage $V_{\overline{M}}$ and current $I_{\overline{M}}$ into the components V_{M1}, V_{M3} and I_{M1}, I_{M3} to satisfy the constraints (12) and (13).

IV. VECTORIAL CONTROL

In steady-state condition, the dynamic equations in (2) are: $\overline{V}_{sk} = -\overline{Z}_{sk}\overline{I}_{sk} - jK_{qk}\omega_m$, $\overline{Z}_{sk} = R_s + j\,k\,p\,\omega_m L_{sk}$. The voltage constraint $\sqrt{V_{dk}^2 + V_{qk}^2} \le V_{Mk}$ in subspace $\overline{\Sigma}_{\omega k}$ with $k \in \{1, 3\}$ can be rewritten as follows:

$$(I_{dk} - X_{0k})^2 + (I_{qk} - Y_{0k})^2 \le R_{0k}^2 \quad (14)$$

where $R_{0k}(\omega_m) = \left|\overline{R}_{0k}\right|_{|\overline{V}_{sk}| = V_{Mk}} = \dfrac{V_{Mk}}{|\overline{Z}_{sk}|}$ (15)

$$X_{0k}(\omega_m) = Re(\overline{C}_{0k}) = -K_{qk}\,k\,p\,\omega_m^2 L_{sk}\,/\,|\overline{Z}_{sk}|^2 \quad (16)$$

$$Y_{0k}(\omega_m) = Im(\overline{C}_{0k}) = -K_{qk}\,\omega_m R_s\,/\,|\overline{Z}_{sk}|^2. \quad (17)$$

Relation (14) is the mathematical expression of the maximum voltage circle $\mathcal{CV}_k$ corresponding to the value V_{Mk} that satisfies the voltage constraint (12). The current vector $\overline{I}_{sk}$ satisfies the voltage constraint only if its modulus is inside the maximum voltage circle $\mathcal{CV}_k$. The terms $\overline{C}_{0k}(\omega_m) =$

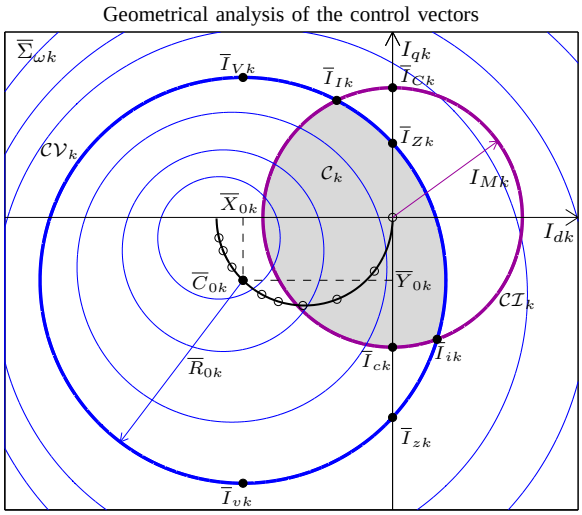

Fig. 4. Maximum current circles $\mathcal{CV}_k$ and $\mathcal{CI}_k$ in subspace $\Sigma_{\omega k}$.

$X_{0k}+j\,Y_{0k}$ and $R_{0k}\,(\omega_m)$ represent the center and the radius of $\mathcal{CV}_k$. When velocity ω_m increases the radius R_{0k} of circle $\mathcal{CV}_k$ decreases and its center $\overline{C}_{0k}$ moves in the complex plane $\overline{\Sigma}_{\omega k}$. The current vector $\overline{I}_{sk}$ must also satisfy the current constraint (13):

$$I_{dk}^2 + I_{qk}^2 \leq I_{Mk}^2 \tag{18}$$

that defines the maximum current circle $\mathcal{CI}_k$. A graphical representation of the voltage and current circles $\mathcal{CV}_k$ and $\mathcal{CI}_k$ on the complex plane $\overline{\Sigma}_{\omega k}$ for a particular value of ω_m is shown in blue and purple in Fig. 4. The intersection zone $\mathcal{C}_k$ of the two circles, shown in grey in Fig. 4, represents the domain in which both the voltage and current constraints are satisfied. Subtracting equation (18) from equation (14) one obtains the following relation:

$$-2X_{0k}I_{dk} - 2Y_{0k}I_{qk} + X_{0k}^2 + Y_{0k}^2 - R_{0k}^2 + I_{Mk}^2 = 0.$$

Using this relation together with (18), one obtains the intersection points $\overline{I}_{Ik}$ and $\overline{I}_{ik}$ of circle $\mathcal{CV}_k$ with circle $\mathcal{CI}_k$:

$$\overline{I}_{I,ik} = \frac{Y_{0k}}{|\overline{C}_{0k}|}\left[\frac{X_{0k}P_k}{|\overline{C}_{0k}|} \pm \sqrt{I_{Mk}^2 - \frac{Y_{0k}^2 P_k^2}{|\overline{C}_{0k}|^2}}\right]\left(1 - j\frac{X_{0k}}{Y_{0k}}\right) + jP_k \tag{19}$$

where $P_k = \frac{|\overline{C}_{0k}|^2 - R_{0k}^2 + I_{Mk}^2}{2Y_{0k}}$.

The coordinates of the other points shown in Fig. 4 are:

$$\overline{I}_{Vk}(\omega_m) = X_{0k}(\omega_m) + jY_{0k}(\omega_m) + jR_{0k}(\omega_m) \tag{20}$$

$$\overline{I}_{Zk}(\omega_m) = jY_{0k}(\omega_m) + j\sqrt{R_{0k}^2(\omega_m) - X_{0k}^2(\omega_m)} \tag{21}$$

$$\overline{I}_{Ck} = jI_{Mk} \tag{22}$$

$$\overline{I}_{vk}(\omega_m) = jY_{0k}(\omega_m) - jR_{0k}(\omega_m) \tag{23}$$

$$\overline{I}_{zk}(\omega_m) = jY_{0k}(\omega_m) - j\sqrt{R_{0k}^2(\omega_m) - X_{0k}^2(\omega_m)} \tag{24}$$

$$\overline{I}_{ck} = -jI_{Mk} \tag{25}$$

The torque can be generated only by the current vectors $\overline{I}_{s1}$ and $\overline{I}_{s3}$ inside the intersection zones $\mathcal{C}_1$ and $\mathcal{C}_3$ of the maximum voltage and current circles $\mathcal{CV}_1$, $\mathcal{CI}_1$ and $\mathcal{CV}_3$, $\mathcal{CI}_3$. Therefore the voltage and current limits determine the torque producing capability of the two subspaces $\overline{\Sigma}_{\omega 1}$ and $\overline{\Sigma}_{\omega 3}$. For a given ω_m it is possible to modulate the components V_{M1}, I_{M1} and V_{M3}, I_{M3} in the subspace $\overline{\Sigma}_{\omega 1}$ and $\overline{\Sigma}_{\omega 3}$ in order to increase or decrease the maximum voltage and current circles $\mathcal{CV}_1$, $\mathcal{CI}_1$ and $\mathcal{CV}_3$, $\mathcal{CI}_3$ satisfying the constraints (12), (13). For the torque control law described in the next section, four different constraints distributions into the subspaces $\overline{\Sigma}_{\omega 1}$ and $\overline{\Sigma}_{\omega 3}$ will be considered, see Fig. 5. The dashed lines are the voltage and current circles $\mathcal{CV}_k$ and $\mathcal{CI}_k$ showed in Fig. 4, while the solid lines are the new circles $\mathcal{CV}'_k$ and $\mathcal{CI}'_k$ obtained modulating the components V_{Mk} and I_{Mk}.

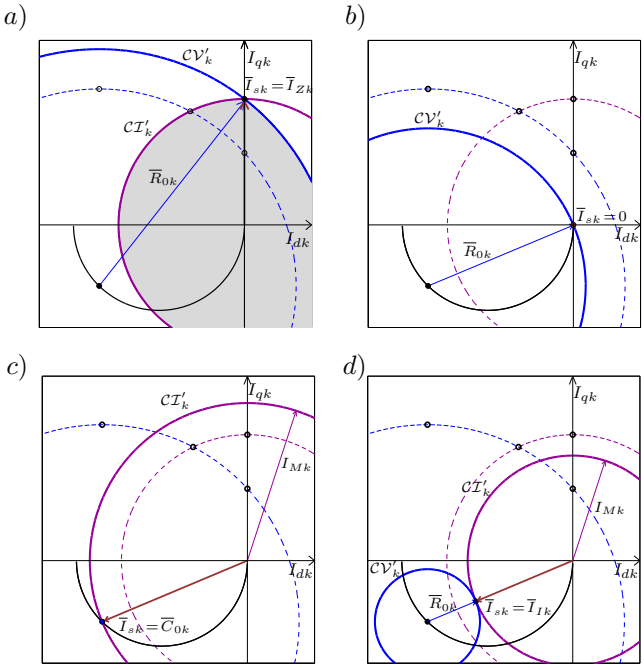

Fig. 5. Maximum current circles $\mathcal{CV}_k$ and $\mathcal{CI}_k$ in subspace $\Sigma_{\omega k}$ obtained modulating the components V_{Mk} and I_{Mk}.

In Fig. 5.a the operation point is $\overline{I}_{sk} = \overline{I}_{Zk} \equiv \overline{I}_{Ck} \equiv \overline{I}_{Ik}$, so the torque can be generated using only the quadrature component I_{qk}. Given the current constraint I_{Mk} and using equations (21) and (22), one obtains the component V_{Mk}:

$$V_{Mk} = |\overline{Z}_{sk}|\sqrt{X_{0k}^2 + (I_{Mk} - Y_{0k})^2}. \tag{26}$$

In Fig. 5.b the operation point is the origin $\overline{I}_{sk} = 0$ because $I_{Mk} = 0$, so the torque generated by subspace $\Sigma_{\omega k}$ is zero. The component V_{Mk} has the following structure:

$$V_{Mk} = |\overline{Z}_{sk}|\,|\overline{C}_{0k}| = K_{qk}\,\omega_m. \tag{27}$$

In Fig. 5.c the operation point is $\overline{I}_{sk} = \overline{C}_{0k}$ because $V_{Mk} = 0$, so the torque generated by subspace $\Sigma_{\omega k}$ is negative. The component I_{Mk} has the following structure:

$$I_{Mk} = |\overline{C}_{0k}| = K_{qk}\,\omega_m \,/\, |\overline{Z}_{sk}|\,. \tag{28}$$

In Fig. 5.d the operation point is $\overline{I}_{sk} = \overline{I}_{Ik} \equiv \overline{I}_{ik}$. Also in this case the torque generated by subspace $\Sigma_{\omega k}$ is negative. Given the current constraint I_{Mk}, from (19) one obtains $R_{0k} + I_{Mk} = |\overline{C}_{0k}|$ and the component V_{Mk} is:

$$V_{Mk} = |\overline{Z}_{sk}|\,(|\overline{C}_{0k}| - I_{Mk}) = K_{qk}\omega_m - |\overline{Z}_{sk}|I_{Mk}. \tag{29}$$

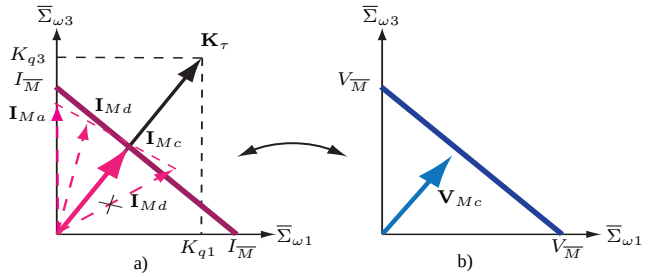

Fig. 6. Minimum dissipation a) current and b) voltage constraints distribution for a 5-phase machine with $K_{q3} > K_{q1}$.

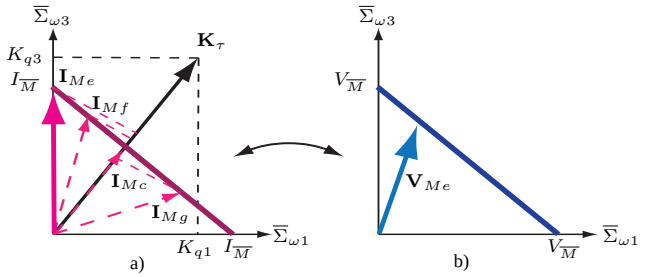

Fig. 7. Maximum torque a) current and b) voltage constraints distribution for a 5-phase machine with $K_{q3} > K_{q1}$.

These four cases show that when the operation point is defined, the components V_{Mk} and I_{Mk} are bounded by the equations (18) and (14).

V. TORQUE CONTROL

Torque τ_m can be controlled by current vectors ${}^{\omega}\overline{\mathbf{I}}_d$ in frame $\overline{\Sigma}_\omega$ not exceeding the constraints on the maximum input voltage and current. When ${}^{\omega}\overline{\mathbf{I}}_d$ is constant, the condition ${}^{\omega}\overline{\mathbf{I}}_s = {}^{\omega}\overline{\mathbf{I}}_d$ can be achieved using the following control:

$$ {}^{\omega}\overline{\mathbf{V}}_s = {}^{\omega}\overline{\mathbf{Z}}_s\, {}^{\omega}\overline{\mathbf{I}}_s + {}^{\omega}\overline{\mathbf{K}}_\tau\, \omega_m - \mathbf{K}_c({}^{\omega}\overline{\mathbf{I}}_s - {}^{\omega}\overline{\mathbf{I}}_d) \qquad (30) $$

where $\mathbf{K}_c > 0$ is a diagonal matrix used for the control design and ${}^{\omega}\mathbf{I}_d$ is obtained as follows:

$$ {}^{\omega}\overline{\mathbf{I}}_d = \begin{cases} {}^{\omega}\overline{\mathbf{I}}_M & \text{if} \quad \tau_d \geq \tau_M(\omega_m) \\ {}^{\omega}\overline{\mathbf{I}}_{cc} & \text{if} \quad \tau_{Md}(\omega_m) < \tau_d < \tau_M(\omega_m) \\ {}^{\omega}\overline{\mathbf{I}}_{md} & \text{if} \quad 0 \leq \tau_d \leq \tau_{Md}(\omega_m) \end{cases} \qquad (31) $$

where τ_d is the desired torque, $\tau_{Md}(\omega_m)$ is the maximum torque with minimum dissipation while $\tau_M(\omega_m)$ is the maximum torque. These two limit torques are function of the motor parameters, the voltage and current constraints and the control law. The desired torque τ_d can be provided using the *minimum dissipation torque control* when $\tau_d \leq \tau_{Md}$ and using the *convex combination torque control* when $\tau_{Md} < \tau_d < \tau_M$. When the desired torque τ_d is greater than the maximum torque τ_M, the *maximum torque control* must be used for satisfying the constraints, in this case the desired torque is saturated to τ_M.
This control law, used together with relation (30), provides the desired torque τ_d satisfying the constraints (12), (13) and minimizing, when possible, the current dissipation.

A. Minimum dissipation torque control

The current constraint vector $\mathbf{I}_M$ which minimizes the power dissipation is the vector with the minimum modulus parallel to vector $\mathbf{K}_\tau$ (see Fig. 6.a). Indeed the scalar product of the four vectors $\mathbf{I}_{Ma}$, $\mathbf{I}_{Mb}$, $\mathbf{I}_{Mc}$ and $\mathbf{I}_{Md}$ with the vector $\mathbf{K}_\tau$ is the same but the vector with minimum modulus is the vector $\mathbf{I}_{Mc}$ parallel to $\mathbf{K}_\tau$. Note that the vector $\mathbf{I}_{Md}$ does not satisfy the current constraint, therefore this distribution cannot be used. The voltage vector $\mathbf{V}_{Mc}$ related to the current vector $\mathbf{I}_{Mc}$ is reported in Fig. 6.b. The current constraint vector $\mathbf{I}_M$ minimizing the power dissipation is:

$$ \mathbf{I}_M = \frac{\tau_d}{|\mathbf{K}_\tau|}\hat{\mathbf{K}}_\tau = \frac{\mathbf{K}_\tau}{|\mathbf{K}_\tau|^2}\tau_d = \begin{bmatrix} \widetilde{K}_1 \\ \widetilde{K}_3 \end{bmatrix} \tau_d \qquad (32) $$

where:

$$ \widetilde{K}_1 = \frac{K_{q1}}{|\mathbf{K}_\tau|^2} = \frac{a_1}{p\varphi_c\sqrt{\frac{5}{2}\left[a_1^2+9a_3^2\right]}}\,,\ \widetilde{K}_3 = \frac{K_{q3}}{|\mathbf{K}_\tau|^2} = \frac{3a_3}{p\varphi_c\sqrt{\frac{5}{2}\left[a_1^2+9a_3^2\right]}} $$

are the distribution coefficients of the current constraint $I_{\overline{M}}$ into the subspaces $\overline{\Sigma}_{\omega 1}$ and $\overline{\Sigma}_{\omega 3}$. Only the quadrature components I_{q1} and I_{q3} of the current vectors $\overline{I}_{s1}$ and $\overline{I}_{s3}$ are used to generate torque (see Fig. 5.a), therefore the current vector ${}^{\omega}\overline{\mathbf{I}}_{md}$ which minimizes the power dissipation is:

$$ {}^{\omega}\overline{\mathbf{I}}_{md} = \begin{bmatrix} j\widetilde{K}_1 \\ j\widetilde{K}_3 \end{bmatrix} \tau_d = \frac{{}^{\omega}\overline{\mathbf{K}}_{\tau N}}{|{}^{\omega}\overline{\mathbf{K}}_{\tau N}|^2}\tau_d \qquad (33) $$

Note that the current vector ${}^{\omega}\overline{\mathbf{I}}_{md}$ is parallel to the torque vector ${}^{\omega}\overline{\mathbf{K}}_{\tau N}$. Substituting (32) in (26) and using the voltage constraint (12), one obtains the following equation:

$$ \underbrace{|\overline{Z}_{s1}|\sqrt{X_{01}^2+(\tau_d\,\widetilde{K}_1-Y_{01})^2}}_{V_{M1}} + \underbrace{|\overline{Z}_{s3}|\sqrt{X_{03}^2+(\tau_d\,\widetilde{K}_3-Y_{03})^2}}_{V_{M3}} = V_{\overline{M}}. \qquad (34) $$

At low velocity the current constraint limits the torque. Using (32) and the current constraint (13) the maximum torque with minimum dissipation at low velocity is:

$$ \tau_{Md}(0) = I_{\overline{M}} \Big/ \left[\widetilde{K}_1 + \widetilde{K}_3\right] $$

Substituting $\tau_{Md}(0)$ in (34) one obtains the rated velocity ω_{rMd}. When $\omega_m > \omega_{rMd}$, the limit torque decreases and it is limited by the voltage constraint. Given $\omega_m > \omega_{rMd}$, equation (34) can be numerically solved with respect to τ_d in order to obtain the maximum torque $\tau_{Md}(\omega_m)$ satisfying minimum dissipation and the voltage and current constraints. The desired torque τ_d can be obtained with minimum current vector ${}^{\omega}\mathbf{I}_{md}$ only if $\tau_d < \tau_{Md}(\omega_m)$.

B. Maximum torque control

The maximum torques $\tau_M(\omega_m)$ can be obtained maximizing the projection of the vector $\mathbf{I}_M$ onto the torque vector $\mathbf{K}_\tau$, see Fig. 7.a. The vectors $\mathbf{I}_{Mc}$, $\mathbf{I}_{Mf}$ and $\mathbf{I}_{Mg}$ do not maximize the torque because their projections onto $\mathbf{K}_\tau$ are smaller than the projection of vector $\mathbf{I}_{Me}$. The vector $\mathbf{I}_M = \mathbf{I}_{Me}$ that maximizes the scalar product $\mathbf{K}_\tau^{\mathrm{T}}\mathbf{I}_M$ is obtained giving the maximum value $I_{\overline{M}}$ to the component I_{M3} related to the maximum component K_{q3} of vector $\mathbf{K}_\tau$. The voltage vector $\mathbf{V}_{Me}$ related to the current vector $\mathbf{I}_{Me}$ is reported in Fig. 7.b.
To reach this goal it is necessary to sort the components K_{q1} and K_{q3} of the vector $\mathbf{K}_\tau$ and apply the following

current and voltage constraints distribution (the reason will be explained later):

$$\begin{cases} I_{Mk} = I_{MG},\ V_{Mk} = |\overline{Z}_{sG}|\sqrt{X_{0G}^2 + (I_{MG} - Y_{0G})^2} & \text{if } k = G \\ I_{Mk} = I_{Mg},\ V_{Mk} = K_{qg}\,\omega_m\ -\ |\overline{Z}_{sg}|\,I_{Mg} & \text{if } k = g \end{cases} \tag{35}$$

where$G$ is the index of the maximum component of $\mathbf{K}_\tau$ and g is the index of the other component of $\mathbf{K}_\tau$.
When $K_{q1} < K_{q3}$ then $g = 1$ and $G = 3$, otherwise when $K_{q1} > K_{q3}$ then $G = 1$ and $g = 3$. The subspace $\overline{\Sigma}_{\omega G}$ related to the maximum component K_{qk} of the torque vector is shown in Fig. 4 and the subspace $\overline{\Sigma}_{\omega g}$ is shown in Fig. 5.d. Note that the component I_{MG} is univocally defined by the current constraint (13): $I_{MG} = I_{\overline{M}} - I_{Mg}$.
Substituting the components V_{Mk} of (35) in the voltage constraint (12) one obtains the following equation:

$$K_{qg}\,\omega_m - |\overline{Z}_{sg}|\,I_{Mg} + |\overline{Z}_{sG}|\sqrt{X_{0G}^2 + (I_{MG} - Y_{0G})^2} = V_{\overline{M}} \tag{36}$$

Given ω_m, equation (36) can be rewritten as:

$$\sqrt{X_{0G}^2 + (I_{\overline{M}} - I_{Mg} - Y_{0G})^2} = \frac{V_{\overline{M}} - K_{qg}\,\omega_m}{|\overline{Z}_{sG}|} + \frac{|\overline{Z}_{sg}|}{|\overline{Z}_{sG}|}\,I_{Mg}$$

This relation can be solved with respect to I_{Mg} obtaining the voltage V_{Mg} of the considered subspaces. The components $\overline{I}_{sk}$ of the maximum current vector ${}^{\omega}\overline{\mathbf{I}}_M$ are univocally defined from the constraints distribution (see Sec. IV):

$${}^{\omega}\overline{\mathbf{I}}_M = \begin{bmatrix} \overline{I}_{s1} \\ \overline{I}_{s3} \end{bmatrix},\ \overline{I}_{sk} = \begin{cases} \max\left\{\overline{I}_{vk}, \overline{I}_{Ik}, \overline{I}_{Zk}\right\} \in \mathcal{C}_k & \text{if } k = G \\ \overline{I}_{Ik} & \text{if } k = g \end{cases} \tag{37}$$

At low velocity the current constraint limits the torque. The maximum value $I_{\overline{M}}$ is given only by the subspace $\Sigma_{\omega G}$ and the equation (35) can be rewritten as:

$$\begin{cases} I_{Mk} = I_{\overline{M}}, V_{Mk} = |\overline{Z}_{sG}|\sqrt{X_{0G}^2 + (I_{\overline{M}} - Y_{0G})^2} & \text{if } k = G \\ I_{Mk} = 0, \quad V_{Mk} = K_{qg}\,\omega_m & \text{if } k = g \end{cases}$$

Note that the component V_{Mg} in the subspace $\overline{\Sigma}_{\omega g}$ it is used to keep the current vector $\overline{I}_{sg}$ equal to zero as it is shown in Fig. 5.b. The maximum torque at low velocity is:

$$\tau_M(0) = p\varphi_c\sqrt{\frac{m_s}{2}}\,G a_G I_{\overline{M}}.$$

When the velocity ω_m increases the components V_{Mg} and V_{MG} increase and there is a velocity ω_{rM} for which the voltage constraint is exactly satisfied. The rated velocity ω_{rM} can be obtained substituting the components V_{Mg} and V_{MG} in (12). When $\omega_m > \omega_{rM}$ the voltage constraint limits the torque then it is necessary to redistribute the current constraint $I_{\overline{M}}$ into the subspace $\overline{\Sigma}_{\omega g}$ to reduce the components V_{Mg}, see (29). Since this operation causes a reduction of the torque (see vector I_{Mf} in Fig. 7.a), the current constraint $I_{\overline{M}}$ is redistributed into the subspaces $\overline{\Sigma}_{\omega g}$ using (35) until $V_{Mg} \geq 0$. At the end, when $V_{Mg} = 0$, the equation (35) can be rewritten as:

$$\begin{cases} I_{Mk} = I_{\overline{M}} - |\overline{C}_{0g}|, V_{Mk} = V_{\overline{M}} & \text{if } k = G \\ I_{Mk} = |\overline{C}_{0g}|, \qquad V_{Mk} = 0 & \text{if } k = g \end{cases}.$$

In this case the component I_{Mg} in the subspace $\overline{\Sigma}_{\omega g}$ is used to keep the component V_{Mg} equal to zero as shown in Fig. 5.c. Using this control the only subspace that generates torque is $\Sigma_{\omega G}$, indeed the current components $\overline{I}_{sg}$ in the other subspace $\Sigma_{\omega g}$ is negative or equal to zero.

C. Convex combination torque control

When $\tau_{Md} < \tau_d < \tau_M$ the two previous control laws cannot be used and the optimal control law which satisfies the constraints (12), (13) and minimizes the current dissipation is quite complex and difficult to be found. In this case the following suboptimal control law is used. The torque τ_d is obtained using the current vector obtained as a convex combination of the maximum current vector ${}^{\omega}\mathbf{I}_M$, see (37), and the maximum current vector with minimum dissipation ${}^{\omega}\mathbf{I}_{Md} = \frac{{}^{\omega}\overline{\mathbf{K}}_\tau}{|{}^{\omega}\overline{\mathbf{K}}_\tau|^2}\,\tau_{Md}$, see (33):

$${}^{\omega}\overline{\mathbf{I}}_{cc} = {}^{\omega}\mathbf{I}_{Md} + \alpha\,({}^{\omega}\mathbf{I}_M - {}^{\omega}\mathbf{I}_{Md})$$

where coefficient α is: $\alpha = \dfrac{\tau_d - \tau_N(\omega_m)}{\tau_M(\omega_m) - \tau_N(\omega_m)}$.

VI. SIMULATION RESULTS

The simulation results described in this section have been obtained in Matlab/Simulink environment considering a motor with the following electrical and mechanical parameters: $m_s = 5$, $p = 1$, $R_s = 2\,\Omega$, $L_s = 0.03$ H, $M_{s0} = 0.025$ H, $a_{M1} = 1$, $a_{M3} = 1/3$, $\varphi_r = 0.02$ Wb, $J_m = 1.6$ kg m^2, $b_m = 0.15$ Nm s/rad, $V_{max} = 100$V, $I_{max} = 35$A $a_1 = 0.8$, $a_3 = 0.2$. The external torque τ_e is zero until $t = 15$ s then $\tau_e = 25$ Nm (see the black dashed line in Fig. 8). The time behaviors of motor velocity ω_m, motor torque τ_m, desired torque τ_d, external torque τ_e and maximum torques τ_M and τ_N are shown in Fig. 8 and the corresponding trajectories on the torque plane (τ_m, ω_m) are reported in Fig. 9. In Fig. 9 the limit torques $\tau_{Md}(\omega_m)$ and τ_M define three zone: the

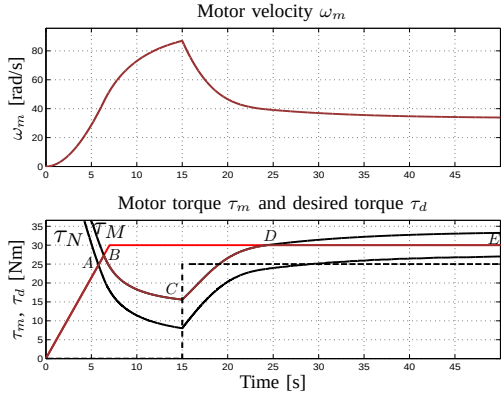

Fig. 8. Time behaviors of motor velocity ω_m, motor torque τ_m (brown), desired torque τ_d (red), external torque τ_e (magenta) and maximum torques τ_M and τ_N (black).

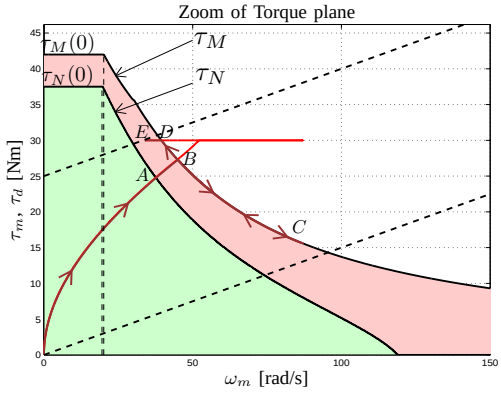

Fig. 9. Motor torque τ_m (brown), desidered torque τ_d (red) and maximum torques τ_M and τ_N (black) as a function of motor velocity ω_m.

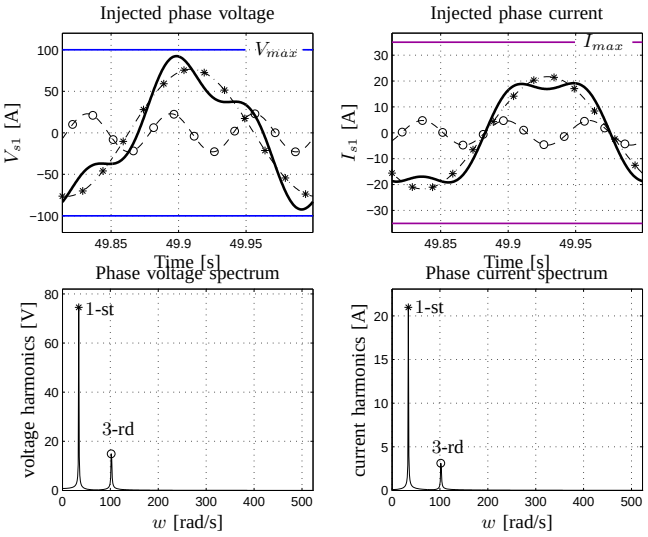

Fig. 10. Phase current and voltage waveform with their corresponding harmonic spectrum in steady-state condition.

green zone represents the region where the desired torque τ_d can be provided minimizing the power dissipation, the red zone represents the region where the desired torque can be provided using the convex combination and the white zone is not allowed. The letters A, B, C, D and E refer to the critical points for the control: A when $\tau_d = \tau_{Md}$, B and D when $\tau_d = \tau_M$, C when the external torque τ_e is applied and E the final steady-state condition. Note that for $\tau_d \leq \tau_M$, i.e. from point 0 to point B and from point D to point E, the control law (30) and (31) guarantees $\tau_m = \tau_d$. Fig. 10 shows the phase current and phase voltage waveforms in the steady-state condition and their corresponding spectrum. It is clear that the phase voltage and current are obtained injecting the 1-st and the 3-rd harmonics. Moreover the obtained current and voltage waveforms satisfy the constraint (10). The constraints (12) and (13) are always satisfied as it is shown in Fig. 11. The current vectors $\overline{I}_{s1}$ and $\overline{I}_{s3}$ in the complex subspaces $\overline{\Sigma}_{\omega 1}$ and $\overline{\Sigma}_{\omega 3}$ are shown in Fig. 12. The desired torque τ_d is provided only by the quadrature components I_{q1} and I_{q3} until it is $\tau_d = \tau_N$ in point A. From point B to point D the maximum torque control ${}^{\omega}\mathbf{I}_M$ is used, the desired torque τ_d is generated only by the current vector

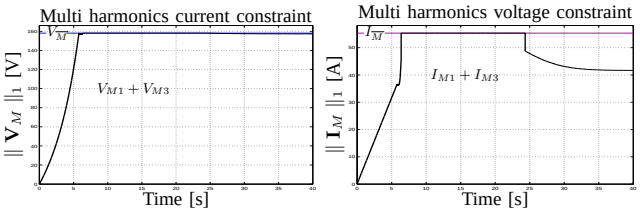

Fig. 11. Time behaviors of the sum of components V_{Mk} and I_{Mk} of vectors $\mathbf{V}_M$ and $\mathbf{I}_M$.

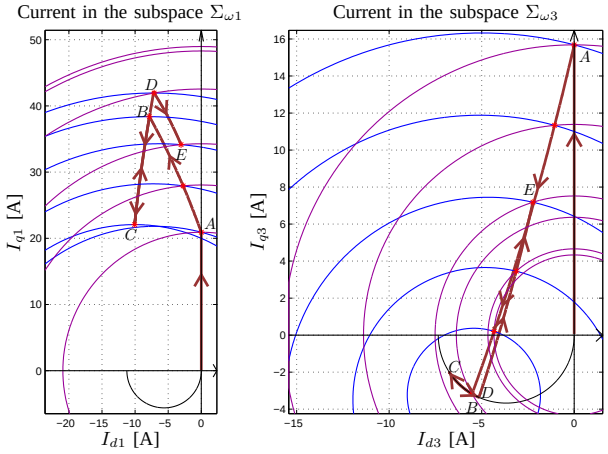

Fig. 12. Current and voltage circles $\mathcal{CV}_k$, $\mathcal{CI}_k$ and current vectors $\overline{I}_{sk}$ in the complex subspaces $\Sigma_{\omega k}$.

$\overline{I}_{s1}$. From A to B and from D to E the desired torque τ_d is provided using also the direct components I_{d1} and I_{d3} of current vectors $\overline{I}_{s1}$ and $\overline{I}_{s3}$.

VII. CONCLUSIONS

In this paper a new vectorial approach to obtain the optimal current references considering the voltage and current constraints has been proposed. The optimality of the control law is guaranteed when the minimum dissipation torque control or the maximum torque control are applied. Simulation results obtained in Simulink for a 5-phase motors validated the effectiveness of the presented control law.

REFERENCES

[1] E. Semail, X. Kestelyn, A. Bouscayrol, "Right Harmonic Spectrum for the Back-Electromotive Force of a n-phase Synchronous Motor", Industry Applications Conference, 2004, 39th IAS Annual Meeting.

[2] L. Parsa and H.A. Toliyat, "Five-Phase Permanent-Magnet Motor Drives", IEEE Tran. on Industry Applications, 2005, Vol. 41, No. 1.

[3] S. Xue, X. Wen, Z. Feng, "Multiphase Permanent Magnet Motor Drive System Based on A Novel Multiphase SVPWM", IPEMC 2006, vol.1.

[4] F. Locment, E. Semail, X. Kestelyn, "Optimum use of DC bus by fitting the back-electromotive force of a 7-phase Permanent Magnet Synchronous machine" , EPE 2005, Dresden, Germany, Sep. 2005.

[5] L. Parsa, N. Kim, H.A. Toliyat, "Field Weakening Operation of a High Torque Density Five Phase Permanent Magnet Motor Drive",IEEE Int. Conference on Electric Machines and Drives, 15 May 2005

[6] R. Zanasi, M. Fei, "Saturated Vectorial Control of Multi-phase Synchronous Motors", NOLCOS 2010 - 8th IFAC Symposium on Nonlinear Control Systems, Bologna, Italy, 1-3 September 2010.

[7] R.Zanasi, F.Grossi, M.Fei, " Complex Dynamic Models of Multi-phase Permanent Magnet Synchronous Motors", IFAC 2011, 18th World Congress, Milano, Italy, 28 August - 2 September 2011.

[8] R. Zanasi, "The Power-Oriented Graphs Technique: system modeling and basic properties", VPPC 2010, Lille, France, Sept 2010.

[9] R. Zanasi, F. Grossi, "Multi-phase Synchronous Motors: POG Modeling and Optimal Shaping of the Rotor Flux", ELECTRIMACS 2008, Québec, Canada, 2008.